

Dendronized Cryptophanes as Water-Soluble Xenon Hosts for ^{129}Xe Magnetic Resonance Imaging

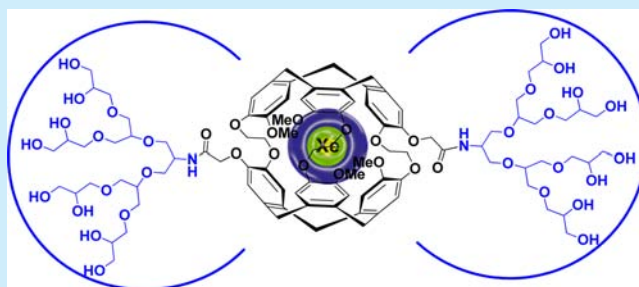
Rahul Tyagi,^{†,§} Christopher Witte,^{‡,§} Rainer Haag,^{*,†} and Leif Schröder^{*,‡}

[†]Institut für Chemie und Biochemie, Freie Universität Berlin, Takustrasse 3, Berlin 14195, Germany

[‡]ERC Project BiosensorImaging, Leibniz-Institut für Molekulare Pharmakologie (FMP), Robert-Roessle-Strasse 10, Berlin, Germany

S Supporting Information

ABSTRACT: Cryptophane cages are very promising for ^{129}Xe -MRI. These molecular cages are extremely hydrophobic, which currently limits their use for diagnostic applications. To overcome this, the synthesis of water-soluble dendronized cryptophanes with surface groups for further functionalization is reported here. These molecules retained all the “core properties of cryptophane” that are crucial for biosensor applications as analyzed by Hyper-CEST imaging and spectroscopy. This approach is promising for developing new generations of xenon–cryptophane-based biosensors.



Since cryptophane cages were first synthesized by Collet and co-workers in 1981, their ability to host molecules and atoms has been well explored. In particular, these molecular cages exhibit a high affinity for xenon. Although xenon is a chemically inert gas, these interactions with cryptophanes have been exploited to “functionalize” xenon.¹ In addition, it can be hyperpolarized using spin-exchange optical pumping,² thereby increasing its detectable signal by 4–5 orders of magnitude in nuclear magnetic resonance (NMR) experiments. Altogether, these properties have led to the development of xenon–cryptophane (Xe@Cry) based biosensor NMR and nuclear magnetic imaging (MRI). Since this concept was first introduced by Pines and co-workers in 2001, extensive research has been performed in this field.³ One particularly important advance in the field was the development of the Hyper-CEST (chemical exchange saturation transfer with hyperpolarized nuclei) detection technique.⁴ This indirect detection technique relies on the exchange of xenon in and out of the host to amplify the Xe@Cry biosensor signal. A selective saturation pulse can only depolarize those xenon nuclei bound in the Xe@Cry complex, thus making them effectively invisible to magnetic resonance detection. With an exchange rate in the range of 10–100/s, a saturation pulse of only a few seconds allows each cage to potentially depolarize thousands of xenon nuclei. This depolarization accumulates in the pool of free xenon nuclei in solution, and it is the depolarization of this pool that is measured after taking a reference measurement without selective saturation.

For the development of Cry–Xe biosensors, cryptophanes and their derivatives have been functionalized with ligands that can bind to a specific target molecule.¹ To increase the capability of Xe biosensors, there have been numerous efforts to make them an effective tool for diagnostic applications.³ Although cryptophanes are attractive candidates for hosting

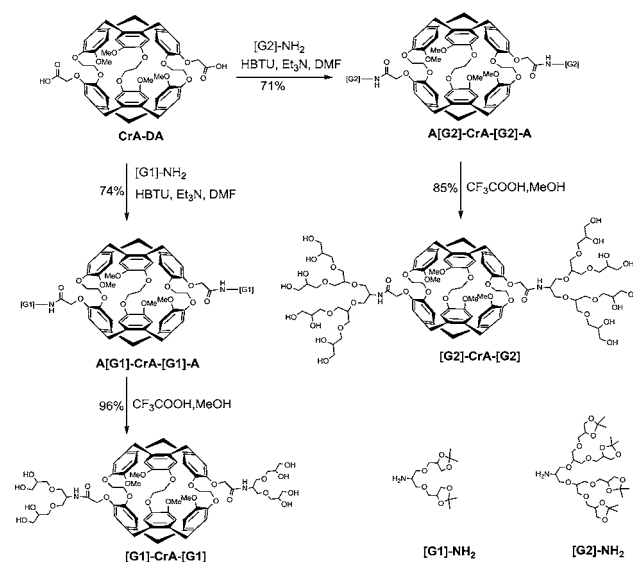
xenon atoms for biosensors, their use has been limited for in vitro or in vivo diagnostic applications because of their high hydrophobicity, which leads to unspecific anchoring into the cell membrane.⁵ In this context, several approaches have been taken to enhance the water solubility of cryptophanes. Cryptophane can be modified/functionalized in a variety of ways to achieve this goal such as metal complexation of cryptophanes,⁶ the core synthesis of cryptophanes possessing a number of polar groups,⁷ and also conjugation of water solubilizing linkers.⁸ Rousseau and co-workers have recently reported the synthesis of a cryptophane core molecule possessing poly(ethylene glycol)s as a water-solubilizing unit and free alkyne groups⁹ that provide room for further functionalization. Although this route clearly provides safe access to this promising cryptophane derivative, the compound was produced in five steps in only 3% overall yield and is therefore lacking in practical applicability. This is also the major drawback of most of the reported routes for producing such molecules. We realized that the grafting of a water-solubilizing linker to cryptophane is a more convenient and promising methodology to enhance its water solubility in order to avoid metal contamination, tedious protection–deprotection multi-step synthesis, etc. Furthermore, there are not many examples of functionalizable cryptophane derivatives that have been produced with the grafting approach and also been evaluated for Xe binding affinity and their suitability for ^{129}Xe Hyper-CEST signal sensitivity. Hence, there is a need for a more convenient and versatile approach for producing such functionalizable, water-soluble cryptophane molecules and their applicability for developing a new generation of Xe@Cry biosensors. Moreover, retaining the core binding and

Received: July 4, 2014

Published: August 25, 2014

exchange properties of molecular cages toward Xe in its water-soluble and functionalizable version is also critical. To achieve this goal, a straightforward synthesis of such cryptophanes was developed by using cryptophane A diacid (CrA-da) and a water-soluble polyglycerol (PG) dendron of generations [G1] and [G2]. In our initial attempts, the dendron coupling to cryptophane was not successful. This includes dendrons carrying hydroxyl, azide, and alkyne functional groups at its focal point to cryptophane carrying acid, alkyne, and azide functional groups, respectively. The conjugation was only achieved through amide formation, particularly by using the HDTU coupling reagent. This is the first report where dendrons have been conjugated to cryptophanes, and high water solubility was achieved using neutral molecules (Scheme 1).

Scheme 1. Synthesis of Dendronized Cryptophanes



Dendrons are well-known for their advantages in biological applications.¹⁰ The nonionic PG dendrons offer distinct advantages in comparison to alternative approaches as they minimize unspecific bindings to biological targets. PG dendrons can be easily synthesized, even in bulk quantities, from inexpensively available glycerol.¹¹ Moreover, PG possesses favorable properties such as high biocompatibility and provides multifunctionality on the outer surface,¹² which can be further functionalized in a regioselective fashion,¹³ thus rendering a promising and versatile approach to advance cryptophanes for designing Cry–Xe-based biosensors that are suitable for biological studies.

The synthesis of dendronized cryptophane molecules was achieved by conjugating CrA-da to the acetal protected, core aminated PG dendrons ([G1]-NH₂ or [G2]-NH₂) as shown in Scheme 1 by using the standard amide bond formation reaction conditions. The resultant acetal-protected dendronized cryptophanes, i.e., A-[G1]-CrA-[G1]-A and A-[G2]-CrA-[G2]-A, were obtained in 71–74% yield as shown in Scheme 1. Subsequent deprotection of the acetal-protected dendronized cryptophanes under acidic conditions with TFA yielded the final dendronized cage molecules [G1]-CrA-[G1] and [G2]-CrA-[G2] in 96% and 86% yields, respectively. All the intermediates and final compounds were structurally characterized by ¹H NMR, ¹³C NMR spectroscopy, and mass

spectrometry. Then the water solubility was investigated for both of the dendronized cage molecules. It was observed that cryptophane diacid conjugated with PG dendron [G1] was partially soluble, but it was completely water-soluble with PG dendron [G2] (Figure 1) as exemplified by their relative Xe NMR signal intensities.

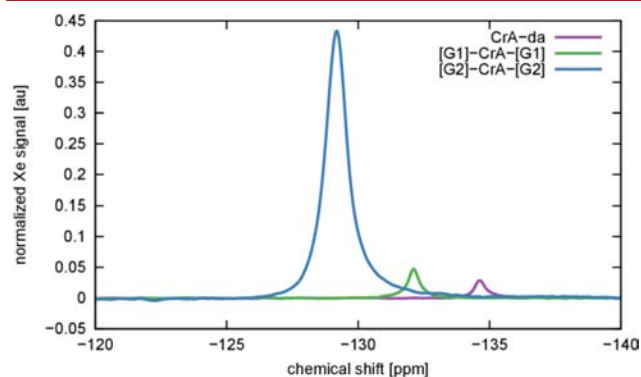


Figure 1. Direct Xe NMR of xenon hosts. Purple: saturated solution of CrA-da (peak at -134.6 ppm). Green: saturated solution of first generation construct [G1]-CrA-[G1] (peak at -132.1). Blue: $890\ \mu\text{M}$ solution of second generation construct [G2]-CrA-[G2] (peak at -129.2). All samples in water +0.01% Antifoam A (Sigma). Spectra were averaged 32 times and are normalized and referenced to the signal from xenon free in solution (intensity 1 at 0 ppm). Each successive generation shifted the Xe@ cage resonance approximately 2.5 ppm toward the resonance of Xe free in solution. The first-generation construct only marginally increased the solubility of the CrA, while the second-generation construct was freely soluble in water.

Our next target was to analyze their affinity toward Xe atoms and ¹²⁹Xe NMR signal sensitivity by using Hyper-CEST NMR spectroscopy. To this end, we recorded a CEST spectrum (also called z-spectrum) of a solution containing both cryptophane A monoacid (CrA-ma, a xenon host commonly used in Hyper-CEST experiments) and the second-generation construct [G2]-CrA-[G2]; see Figure 2.

For each data point in the CEST spectrum, xenon was delivered into solution and then a saturation pulse applied (of

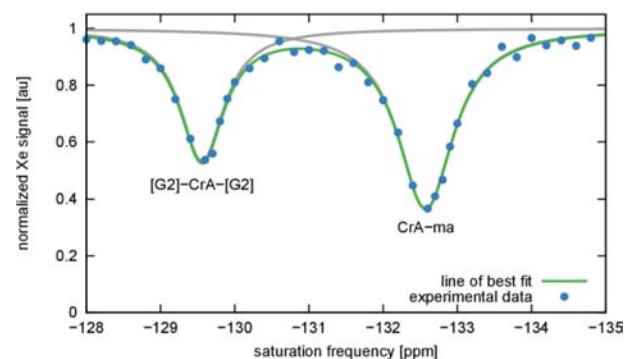


Figure 2. Hyper-CEST spectroscopy of [G2]-CrA-[G2] and CrA-ma in water +0.01% Antifoam A (Sigma) and 0.27% DMSO. Both xenon hosts are at an approximate concentration of $13\ \mu\text{M}$. The saturation frequency is relative to the frequency of free xenon in solution at 0 ppm. The data was fit using a negative exponential of the sum of two Lorentzians¹⁴ (green lines, see the Supporting Information for more details). The contribution from each of the individual Lorentzians is shown with a gray line.

fixed power and duration) which was followed by a read-out of the magnetization of the free xenon in solution. The saturation frequency was systematically varied across the range of interest, in this case, over the two resonances from CrA-ma and the [G2]-CrA-[G2] construct. As the saturation frequency approached one of the resonances, more xenon was depolarized and led to a dip in the spectrum. The exact shape of the CEST-spectrum is determined by the exchange rates, occupancy of the hosts, saturation power, and duration and relaxation rates of xenon. Using a low power continuous wave saturation pulse, we could successfully resolve the two different xenon hosts in a Hyper-CEST spectrum (saturation with $0.65\ \mu\text{T}$, 12 s) and Hyper-CEST image ($1.5\ \mu\text{T}$, 8 s).

As can be seen, the CEST response from the two different hosts is comparable in both spectroscopy, Figure 2, and imaging, Figure 3. Using inversion recovery experiments¹⁵ (see

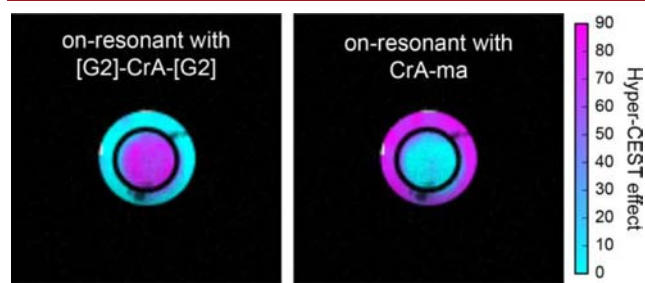


Figure 3. Hyper-CEST images of a double phantom containing [G2]-CrA-[G2] (inner compartment) and CrA-ma (outer compartment), both in water + 0.01% Antifoam A (Sigma) and 0.27% DMSO and overlaid proton reference images. Both xenon hosts are at an approximate concentration of $13\ \mu\text{M}$. The Hyper-CEST images were calculated from a Hyper-CEST image series (with varying saturation frequency) that was denoised using principal component analysis (PCA);¹⁴ see the Supporting Information for more details. When on-resonant with [G2]-CrA-[G2] (left) the Hyper-CEST effect correctly localizes the construct to the inner compartment and when on-resonant with CrA-ma (right) the Hyper-CEST effect correctly localizes the construct to the outer compartment.

the Supporting Information for more details), we could estimate the exchange rate from xenon in a particular host to xenon free in solution. Additionally, we calculated the binding constant using the relative peak areas in the direct spectrum. For Hyper-CEST experiments, these parameters are critical as they determine the strength of the CEST effect. For [G2]-CrA-[G2] and CrA-ma these rates are approximately 23 and 24 per second, and the binding constants are 2750 and $3200\ \text{M}^{-1}$, respectively. This agrees well with exchange rates measured using saturation recovery on similar CrA derivatives in water. This means the addition of the dendrons does not significantly alter the exchange and binding of xenon to the host. This is further confirmed by the similarity of the CEST responses in both imaging and spectroscopy.

Further targeting of these dendronised CrA can be achieved using a number of different techniques.¹³ It can be said that these techniques may produce a statistical admixture of final products that would in turn produce multiple peaks in the xenon spectrum and may complicate analysis in vitro. Nevertheless, at the powers needed in cellulose and in vivo (more than 1 order of magnitude greater than the powers used in this study), these multiple peaks would most likely be so broad that only one peak could be observed. In fact such

admixture of targeted CrA have already been successfully used for Hyper-CEST imaging in cellulose.¹⁶

In summary, we designed and synthesized dendronized cryptophane cage molecules for ^{129}Xe MRI applications. The dendronized cryptophane composed of cryptophane diamide with two [G2] PG dendron was found to be completely water-soluble and could thus serve as a building block for targeted biosensors. It retained all the core properties “of a cryptophane” cage that are crucial for biosensor applications. We believe that the dendronization of cryptophanes is a convenient, versatile, and promising approach for developing a new generation of Cry-Xe-based biosensors.

■ ASSOCIATED CONTENT

Supporting Information

Experimental methods and techniques, experimental procedure of synthesized compounds of Scheme 1 and their characterization data, copies of ^1H and ^{13}C NMR spectra of new compounds. This material is available free of charge via the Internet at <http://pubs.acs.org>.

■ AUTHOR INFORMATION

Corresponding Authors

*Tel: (+49) 30 838 52633. Fax: (+49) 30 838 53357. E-mail: haag@chemie.fu-berlin.de.

*Tel: (+49) 30 947 93121. E-mail: lschroeder@fmp-berlin.de.

Author Contributions

§These authors contributed equally to this work

Notes

The authors declare no competing financial interest.

■ ACKNOWLEDGMENTS

This work has been supported by the Helmholtz Association through the Helmholtz-Portfolio Topic “Technology and Medicine”, the European Research Council under the European Community’s Seventh Framework Programme (FP7/2007-2013)/ERC grant agreement no. 242710, and the Human Frontier Science Program. Furthermore, Dr. Carlo Fasting (Institut für Chemie und Biochemie Organische Chemie Freie Universität Berlin, Takustrasse 3, Berlin 14195, Germany) is thanked for providing the HPLC facility and also for his assistance in the purification of compounds A-[G1]-CrA-[G1-A] and A-[G2]-CrA-[G2]-A.

■ REFERENCES

- (1) Spence, M. M.; Ruiz, E. J.; Rubin, S. M.; Lowery, T. J.; Winssinger, N.; Schultz, P. G.; Wemmer, D. E.; Pines, A. *J. Am. Chem. Soc.* **2004**, *126*, 15287–15294.
- (2) Walker, T. G.; Happer, W. *Rev. Mod. Phys.* **1997**, *69*, 629–642.
- (3) (a) Goodson, B. M. *J. Magn. Reson.* **2002**, *155*, 157–216.
- (b) Schröder, L. *Physica Medica – Eur. J. Med. Phys.* **2013**, *29*, 3–16.
- (4) Schröder, L.; Lowery, T. J.; Hilty, C.; Wemmer, D. E.; Pines, A. *Science* **2006**, *314*, 446–449.
- (5) Boutin, C.; Stopin, A.; Lenda, F.; Brotin, T.; Dutasta, J. P.; Jamin, N.; Sanson, A.; Boulard, Y.; Leteurtre, F.; Huber, G.; Bogaert-Buchmann, A.; Tassali, N.; Desvaux, H.; Carrière, M.; Berthault, P. *Bioorg. Med. Chem.* **2011**, *19*, 4135–4143.
- (6) Fairchild, R. M.; Joseph, A. I.; Holman, K. T.; Fogarty, H. A.; Brotin, T.; Dutasta, J.-P.; Boutin, C.; Huber, G.; Berthault, P. *J. Am. Chem. Soc.* **2010**, *132*, 15505–15507.
- (7) (a) Bai, Y.; Hill, P. A.; Dmochowski, I. J. *Anal. Chem.* **2012**, *84*, 9935–9941. (b) Dubost, E.; Kotera, N.; Garcia-Argote, S.; Boulard, Y.; Léonce, E.; Boutin, C.; Berthault, P.; Dugave, C.; Rousseau, B. *Org.*

Lett. **2013**, *15*, 2866–2868. (c) Hill, P. A.; Wei, Q.; Troxler, T.; Dmochowski, I. J. *J. Am. Chem. Soc.* **2009**, *131*, 3069–3077.

(8) (a) Traore, T.; Clave, G.; Delacour, L.; Kotera, N.; Renard, P.-Y.; Romieu, A.; Berthault, P.; Boutin, C.; Tassali, N.; Rousseau, B. *Chem. Commun.* **2011**, 47, 9702–9704. (b) Seward, G. K.; Bai, Y.; Khan, N. S.; Dmochowski, I. J. *Chem. Sci.* **2011**, *2*, 1103–1110. (c) Chambers, J. M.; Hill, P. A.; Aaron, J. A.; Han, Z.; Christianson, D. W.; Kuzma, N. N.; Dmochowski, I. J. *J. Am. Chem. Soc.* **2008**, *131*, 563–569. (d) Wei, Q.; Seward, G. K.; Hill, P. A.; Patton, B.; Dimitrov, I. E.; Kuzma, N. N.; Dmochowski, I. J. *J. Am. Chem. Soc.* **2006**, *128*, 13274–13283.

(9) Delacour, L.; Kotera, N.; Traoré, T.; Garcia-Argote, S.; Puente, C.; Leteurtre, F.; Gravel, E.; Tassali, N.; Boutin, C.; Léonce, E.; Boulard, Y.; Berthault, P.; Rousseau, B. *Chem.—Eur. J.* **2013**, *19*, 6089–6093.

(10) Gupta, S.; Tyagi, R.; Parmar, V. S.; Sharma, S. K.; Haag, R. *Polymer* **2012**, *53*, 3053–3078.

(11) Burakowska, E.; Haag, R. *Macromolecules* **2009**, *42*, 5545–5550.

(12) Calderón, M.; Quadir, M. A.; Sharma, S. K.; Haag, R. *Adv. Mater.* **2010**, *22*, 190–218.

(13) Malhotra, S.; Calderon, M.; Prasad, A. K.; Parmar, V. S.; Haag, R. *Org. Biomol. Chem.* **2010**, *8*, 2228–2237.

(14) Döpfert, J.; Witte, C.; Kunth, M.; Schröder, L. *Contrast Media Mol. Imaging* **2014**, *9*, 100–107.

(15) Zaiss, M.; Schnurr, M.; Bachert, P. J. *Chem. Phys.* **2012**, *136*, 11697–11702.

(16) Rose, H. M.; Witte, C.; Rossella, F.; Klippel, S.; Freund, C.; Schröder, L. *Proc. Natl. Acad. Sci. U.S.A.* **2014**, *111*, 11697–11702.